Green Chemistry

Accepted Manuscript

This article can be cited before page numbers have been issued, to do this please use: S. Dabral, J. Engel, J. Mottweiler, S. Spoehrle, C. W. Lahive and C. Bolm, *Green Chem.*, 2017, DOI: 10.1039/C7GC03110F.

Volume 18 | Number 7 | 7 April 2016 | Pages 1821–2242

Green Chemistry

Cutting-edge research for a greener sustainable future
www.rsc.org/greenchem

ISSN 1463-9262

ROYAL SOCIETY OF CHEMISTRY

CRITICAL REVIEW
G. Chatel et al.
Heterogeneous catalytic oxidation for lignin valorization into valuable chemicals: what results? What limitations? What trends?

175 YEARS

View Article Online
DOI: 10.1039/C7GC03110F

Journal Name

ARTICLE

Mechanistic studies of base-catalysed lignin depolymerisation in dimethyl carbonate

Received 00th January 20xx,
Accepted 00th January 20xx

DOI: 10.1039/x0xx00000x

www.rsc.org/

Saumya Dabral,[a] Julien Engel,[a] Jakob Mottweiler,[a] Stephanie S. M. Spoehrle,[a,b] Ciaran W. Lahive[b] and Carsten Bolm*[a]

The depleting fossil reservoirs have stimulated global research initiatives on the renewable feedstocks of lignin as sustainable alternatives for petroleum-derived aromatics. Base-catalysed depolymerisation (BCD) is regarded as an economical and efficient approach for the valorisation of technical lignins. The major limiting factor encountered during this process is the re-condensation of the formed phenolic products, which results in lower monomer yields. To diminish these side reactions, we selected alkali earth metal catalysts in dimethyl carbonate (DMC) to produce methylated phenol derivatives as the final products. Herein we demonstrate for the first time a base-promoted depolymerisation process affording low-molecular weight oils in high yields (52-67 wt%) wherein the employed bases are used in truly catalytic quantities (with catalyst loadings of around 5 mol %). The general applicability of this methodology was proven on four different lignin samples (1 Kraft, 3 Organosolv) using caesium carbonate and lithium *tert*-butoxide as catalysts. The 2D NMR on the post reaction lignin samples showed a similar degradation of the major lignin linkages for both bases. A difference for the reduction of phenolic moieties was revealed by quantitative ^{31}P NMR analysis. Furthermore, GPC analysis demonstrated a significant shift towards lower mass fragments for the Cs_2CO_3-catalysed lignin degradation. A detailed GC-MS analysis for these samples identified a range of methoxy capped-monomeric degradation products. The scope of this reaction system was further expanded onto lignocellulosic biomass such as milled beechwood chips, which notably showed similar product distributions. Based on the correlation of the experimental observations for extracted lignin samples and model compound studies, a mechanistic pathway for the Cs_2CO_3-catalysed system was suggested. DFT calculations provided reaction pathways for the observed cleavage products.

Introduction

Lignin is a renewable biopolymer rich in aromatics which represents a considerable portion (roughly 30% on a weight basis and 40% on an energy basis) of the lignocellulosic biomass.[1] Despite being widely available as a waste product from the pulp and paper industry, lignin is by far the least utilised fraction in lignocellulose in comparison to cellulose and hemicelluloses.[2] The structural diversity and complexity of this three-dimensional, amorphous lignin biopolymer attributes to its overall recalcitrance. This represents a major hindrance for obtaining high-value chemicals in an integrated biorefinery. Thus, the lignin fractions are most often relegated to low-value uses and burnt to get energy.[2,3] Since in the forthcoming years biorefineries will process considerable amounts of renewable feedstocks, it becomes important to find efficient valorisation routes and upgrade this readily available resource to make the overall process more economical.[2,3a]

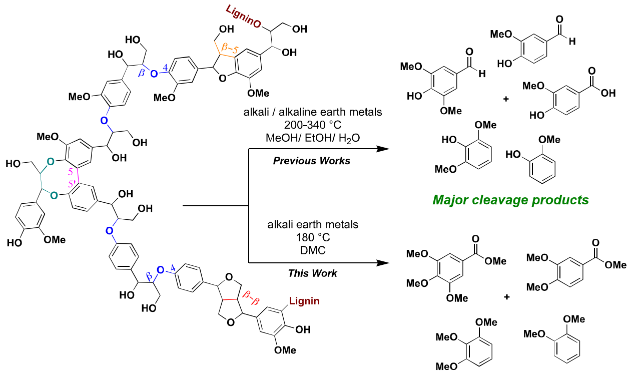

Scheme 1 Base-catalysed cleavage of lignin in DMC.

The lignin structure is composed of a randomly branched network of electron rich phenylpropanols (coumaryl, coniferyl, sinapyl alcohols) that are connected to each other through a variety of stable C-C and etheral C-O linkages.[4] Amongst these, the β-O-4 linkages (Scheme 1) are the most predominant alkyl-aryl ether interconnecting bonds.[2-4] A controlled and selective

---

[a] Institute of Organic Chemistry, RWTH Aachen University, Landoltweg 1, D-52056 Aachen, Germany.
[b] School of Chemistry and Biomedical Science Research Complex, University of St Andrews and EaStCHEM, North Haugh, St Andrews, Fife KY16 9ST, United Kingdom.
Present address: (J. E.: School of Chemistry, Cardiff University, Main Building, Park Place, Cardiff, CF10 3AT, United Kingdom, J. M.: Instituto de Tecnologia Química, (UPV-CSIC), Av de los Naranjos s/n, Valencia SPAIN)

† Electronic Supplementary Information (ESI) available: See DOI: 10.1039/x0xx00000x

View Article Online
DOI: 10.1039/C7GC03110F

Table 1 Characterisation of lignin samples by GPC and 2D-HSQC NMR.

Lignin source	Mw (Da)[a]	S, G, H (%)[b]	β-O-4-OH[c]	Linkages (per 100 C9 units)[b]		
				β-O-4-OR[d]	β-5	β-β
OS-O	2610	85, 14, trace	27	6	3	5
OS-BW	3103	73, 27, trace	20	4	3.2	5.1
OS-C	15220	86, 14, trace	37	1.4	2	6
Aldrich-Kraft	7106	trace, 100, trace	5	0	1	1

[a] Determined by GPC (DMF/LiCl) using RI detector with respect to polystyrene standards. [b] Determined by 2D-HSQC NMR by comparing the aliphatic and aromatic signal intensities (Electronic Supplementary Information 2.2 a). [c] Amounts of β-O-4 linkages with free α-OH. [d] Amounts of β-O-4 linkages with capped α-OH units.

Table 2 Quantitative ^{31}P NMR measurements of the aliphatic, phenolic, and carboxylic hydroxyl groups in lignin samples.[a]

Lignin source	OH (mmol/g)					
	Aliphatic OH	5-substituted OH	guaiacyl OH (G)	*p*-hydroxyphenyl OH (H)	total phenolic OH	COOH
OS-O	2.37	1.06	0.56	0.05	1.66	0.12
OS-BW	2.38	1.24	0.69	0.01	1.94	0.01
OS-C	1.90	1.70	0.88	0.03	2.63	0.07
Aldrich-Kraft	1.79	0.90	1.77	0.17	2.84	0.20

[a] Lignin samples phosphitylated with 2-chloro-4,4,5,5-tetramethyl-1,3,2-dioxaphospholane (Electronic Supplementary Information 2.2.b)

lignin depolymerisation strategy targeting these β-O-4 linkages is a key way for producing a variety of high-value, low molecular weight aromatics.[5] Numerous publications in recent years been devoted to such strategies involving oxidative,[5,6] reductive,[7] redox-neutral,[5c,8] acid-[9] and base-catalysed[10-11] degradation of lignin β-O-4 model compounds and extracted lignin samples. Most of the literature on BCD highlight the advantage of using cheap and readily available reagents (NaOH, KOH, Ca(OH)$_2$, LiOH, liq. NH$_3$ etc.).[10] Lately, in order to make processes more economically viable, there have been attempts to perform the degradation reactions using solid bases that are frequently combined with other metal catalysts.[11] Along those lines a recent article by Chaudhary and Dhepe compared the efficiency for lignin depolymerisation using a variety of heterogeneous bases.[11g] The highest yields for the low molecular weight products (monomers to trimers, 51%) were attained using NaX zeolites at 250 °C with a reaction time of 1 h. It is noteworthy, however, that the base was employed in stoichiometric amounts and a significantly decreased yields for low molecular weight products (monomers to trimers) was observed (51% to 34%) in the first recycle run.[11g]

The use of stoichiometric amounts of base in BCD relative to monomer units present in lignin is a common theme in literature.[10b-c,j-k,m,q] The catalyst loadings are generally given in wt% relative to the weight of solvent and not lignin.[10b-l,n,q] For example, one standard reaction condition entails 10% [w(lignin)/w(solvent)] lignin loading and 2% to 4% [w(base)/w(solvent)] catalyst loading using a base such as NaOH.[10c,i-k,q] The catalyst loadings relative to lignin are therefore usually between 20 wt% and 40 wt%. The majority of BCD reactions require elevated temperatures from 200 °C to 340 °C and are often accompanied by high pressures. Furthermore, these conditions promote secondary reactions between the reactive phenolic and aldehyde/ketone intermediates hence leading to an overall decrease in monomer yields. To obtain higher yields for the monomer rich oil fractions at higher temperature and pressure conditions, Lercher and Toledano independently reported boric acid and phenols as suitable capping agents.[10j,l] Alternatively, we have exploited the versatile chemical nature of DMC at elevated temperatures (> 90 °C) in the presence of bases, and reported a BCD strategy for a range of lignin β-O-4 model compounds obtaining methoxy-capped phenolic and benzoic acid derivatives as products.[10p] Recently, Barrett *et al.* also demonstrated the intricate role of a MeOH/DMC solvent system which helped to increase the aromatic yields by *O*-methylation of the phenolic intermediates for their Cu$_{20}$PMO-catalysed reductive lignin disassembly pathway.[7i]

Predicting the reaction behaviour of real lignin based on results from lignin model compound studies is often not reliable because they frequently differ from each other.[4b,c] Considering these implications, the current study focuses on the BCD of four lignin polymers, aiming to increase the yields of the oil fractions with a higher composition of methoxy-capped low molecular weight products. After having established that the same types of products are formed from lignin as in model compound-based studies, efforts were put in to studying the mechanistic aspects of the reaction. We herein propose reaction pathways leading to the formation of the observed capped-methoxy-aromatics.

Results and Discussion

Characterisation of lignins

In this study, four lignin samples namely three organosolv lignins, isolated from cherry (OS-C), oak (OS-O), beechwood (OS-BW), and commercially available Kraft lignin from Sigma Aldrich (370959) were evaluated under our BCD reaction conditions in DMC. Since the isolation process of a lignin sample significantly influences the physical and chemical properties of the polymer including the identity and ratio of

View Article Online
DOI: 10.1039/C7GC03110F

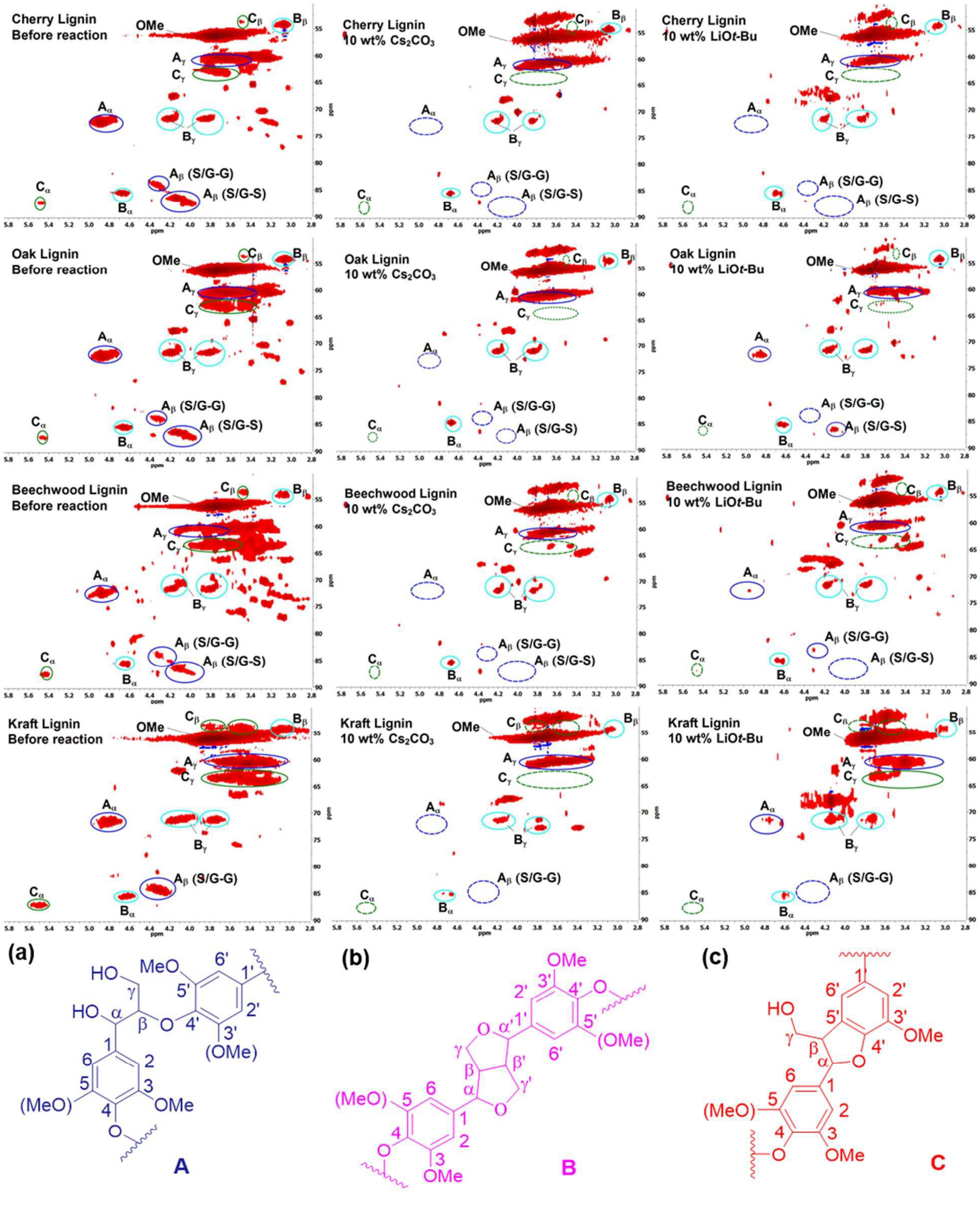

Fig. 1 2D-HSQC NMR spectra (in DMSO-d_6) of organosolv, cherry, oak, beechwood and Aldrich-Kraft lignin; before the reaction; after the reaction with Cs_2CO_3 at 180 °C; after the reaction with LiO*t*-Bu at 180 °C; (a) β-O-4′ aryl ether linkages (b) resinol substructures formed by β–β ′, α-O-γ′, and γ-O-α′ linkages; (c) phenylcoumaran substructures formed by β-5′ and α-O-4′ linkages.

the chemical linkages, the lignin samples were characterised by 2D-HSQC NMR, GPC and ^{31}P NMR [after derivatisation with the phosphorylating agent 2-chloro-4,4,5,5-tetramethyl-1,3,2-dioxaphospholane (TMDP)] measurements prior to usage. These methods were used to determine the abundance of β-O-4, β-5 and β-β linkages as well as to quantify the total amounts of aliphatic hydroxyl groups present in the individual lignin samples. The data from these experiments are outlined in Tables 1 and 2.

View Article Online
DOI: 10.1039/C7GC03110F

Lignin Degradation Studies

The lignin samples were subjected to BCD studies using 10 wt% [w(base)/w(lignin)] of either of the two bases (Cs_2CO_3 or LiO*t*-Bu) at 180 °C for 8 h (Cs_2CO_3) or 12 h (LiO*t*-Bu). Depending on the lignin source this corresponded to a catalyst loading of 5 to 6 mol% for Cs_2CO_3 and 23 to 26 mol% for LiO*t*-Bu. The resulting reaction mixtures were analysed by 2D-HSQC NMR, quantitative ^{31}P NMR and GPC. Lower molecular weight fractions (oil) were separated from the residual lignins by solvent extraction using ethyl acetate and analysed by GC-MS to identify and individually quantify the capped-aromatic monomer products.

2D NMR Studies

Preliminary studies to determine the changes in lignin structures mainly focused on their two-dimensional ^{1}H-^{13}C correlation NMR spectroscopy (HSQC) before and after the BCD reactions. In particular, the aliphatic oxygenated side chain regions (δ_C/ δ_H 50.0-90.0/2.5-5.8) of the HSQC spectra showed a major decrease in the regions corresponding to the β-aryl-ether (β-O-4) and phenylcoumaran (β-5) bonds. The resinol (β-β) linkages seemed to remain unaltered for both the Cs_2CO_3 and LiO*t*-Bu-catalysed BCD processes in all four lignin samples (Fig. 1). A follow up reaction using model compound **1a** further confirmed the low reactivity of the resinol (β-β) linkages for our reaction system (Scheme 2). This could in turn be attributed to the lack of aliphatic hydroxy groups, which were later proven during the mechanistic studies to have a considerable influence on the overall degradation pathway.

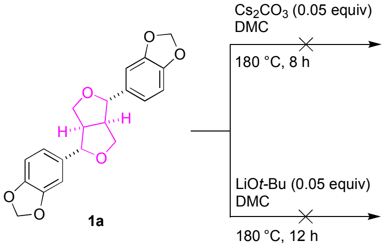

Scheme 2 Reactivity of β-β model compound **1a** in the BCD reactions.

Quantitative ^{31}P NMR Studies

The degradation of the lignin linkages as observed in the 2D-NMR studies prompted us to further investigate its implications for the functional groups still present in the lignin structures. Thus, a series of product analyses were carried out using quantitative ^{31}P NMR spectroscopy in the presence of a known amount of an internal standard (Fig. 2, Table 3).[12] As seen in Fig. 2, for both bases an overall reduction in the amounts of aliphatic, phenolic, and carboxylic -OHs in the lignin samples was observed. However, quantification studies revealed that the Cs_2CO_3-catalysed reactions underwent a complete removal of these functional groups (Table 3 and Table S1). One likely reason for the decrease in aliphatic -OH groups can be credited to the transesterification reaction with DMC catalysed by both the employed bases as shown in Scheme 3. Reports in literature suggest that the various phenolic-OH groups can undergo base promoted methylation.[7h,13] Additionally, the cleavage of the interconnecting bonds could also result in the decreased peak intensities in the defined regions of the spectra. Therefore, follow-up experiments focused on determining any shifts in the average molecular weights of the residual lignin mixtures after BCD reactions.

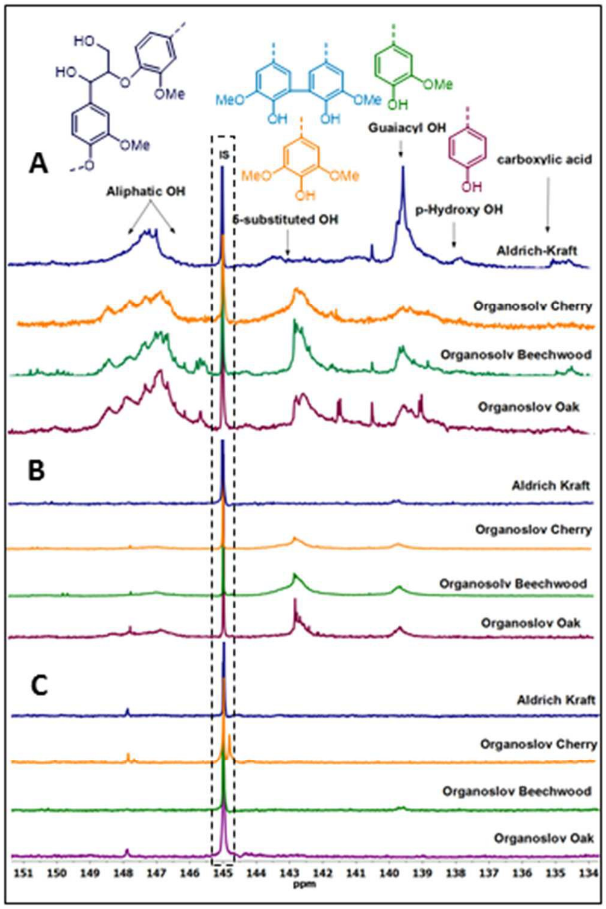

Fig. 2 Quantitative ^{31}P NMR spectra of lignins; **A** before the reaction; **B** after the reaction with LiO*t*-Bu; **C** after the reaction with Cs_2CO_3.

Table 3 Reduction in hydroxyl groups of lignins quantified by ^{31}P NMR using cyclohexanol as internal standard.

Base	% reduction in -OH			
	lignin	aliphatic- OH	5- substitutes OH	guaiacyl OH
LiO*t*-Bu	OS-O	84	48	73
	OS-BW	89	68	74
	OS-C	92	64	74
	Kraft	96	93	93
Cs_2CO_3	OS-O	98	98	97
	OS-BW	99	97	98
	OS-C	97	98	97
	Kraft	99	99	94

View Article Online
DOI: 10.1039/C7GC03110F

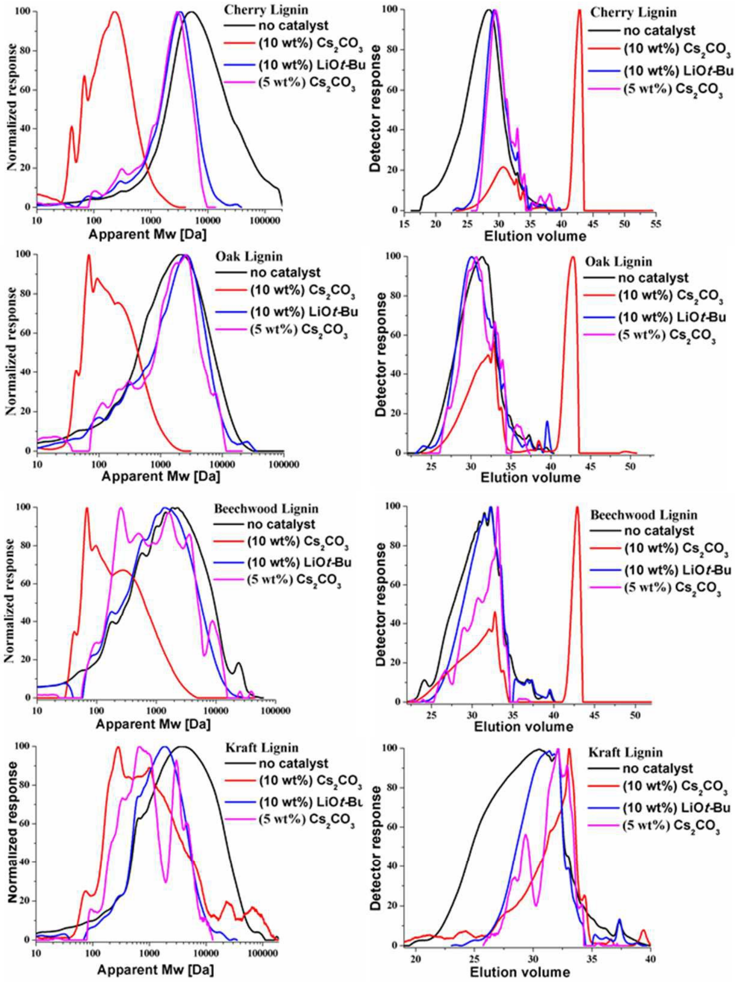

Fig. 3 GPC measurements for the cherry, oak, beechwood and Kraft lignin samples: before reaction (no catalyst); after reaction with Cs_2CO_3 (10 wt%, 0.030 mmol), 8 h, 180 °C; after reaction with LiO*t*-Bu (10 wt%, 0.125 mmol), 12 h, 180 °C; after reaction with Cs_2CO_3 (5 wt%, 0.015 mmol), 8 h, 180 °C. **Left**: mass distribution with respect to polystyrene standards calibration; **Right**: elugram.

Table 4 Average molecular weight change before and after the reactions.

Lignins	Mw (Da)			
	before the reaction	5 wt% Cs_2CO_3	10 wt% Cs_2CO_3	10 wt% LiO*t*-Bu
Organosolv-cherry	15220	2436	253	3235
Organosolv-oak	2610	2022	212	2506
Organosolv-beechwood	3103	2008	383	1898
Aldrich-Kraft	7106	2192	1696	5790

Gel Permeation Chromatography Analysis

The relative change in the weight average molecular weight (M_w) for the lignin samples preceding the BCD was determined by GPC analysis. Fig. 3 depicts the mass distribution chromatograms and the elugrams for the lignins both before and after the BCD with 10 wt% [w(base)/w(lignin)] of Cs_2CO_3 and LiO*t*-Bu under the given reaction conditions. As reflected in Table 4, there was a stark decrease in the M_w values for all the samples treated with Cs_2CO_3 (10 wt%, Fig. 3, red lines), in comparison to the corresponding LiO*t*-Bu-catalysed reactions (Fig. 3, blue lines). For the organosolv lignins, the decrease in mass was more significant in comparison to the Kraft lignin. This can be attributed to the rather condensed structure of Kraft lignin with less alkyl-aryl ether linkages resulting from the more invasive pre-treatment conditions. Furthermore, reactions with reduced amounts of Cs_2CO_3 (5 wt%) proved to be less effective as observed in the GPC (pink lines) thereby emphasising the effect of base concentration on the product outcome. The influence of the base loading did not become apparent through previous HSQC measurements considering that the degradation of the alkyl-aryl ether linkages was already observed with 5 wt% of Cs_2CO_3 and 1.2 wt% of LiO*t*-Bu,[10p] illustrating the importance of various analytical techniques for the characterisation of lignin depolymerisation.

View Article Online
DOI: 10.1039/C7GC03110F

Table 5 Quantification of selected methoxy-capped aromatic monomers identified in the oils obtained after the depolymerisation of lignin samples (OS-OL, OS-CL, OS-BWL, KL = 100 mg) at 180 °C for 8 h with 10 wt% [w(base)/w(lignin)] of Cs_2CO_3 in DMC (5 mL).

Capped monomers	OS-OL	OS-CL	OS-BWL	KL	KL^a
	wt% of starting material				
	0.03	0.02	0.05	0.3	0.2
	0.2	-	0.1	0.05	-
	0.6	0.9	1.1	1.8	1.5
	3.4	4.0	3.2	-	-
total (2+3)	4.23	4.92	4.45	2.15	1.7

^{a} Reaction with 10 wt% [w(base)/w(lignin)] of KOH

GC-MS Analysis

Based on the GPC results, reactions catalysed by 10 wt% of Cs_2CO_3 showed the highest reduction in molecular weight with a M_w value in the range of aromatic monomers and oligomers (200-1900 Da) for the four lignin samples (Table 4). The identification and quantification of these products was thus sought to be done by GC-MS analysis of the low-molecular weight oil fractions (52-67%) [w(oil)/w(initial lignin)] obtained after its separation from the ethyl acetate insoluble residue of the reaction mixture (for further details see Electronic Supplementary Information section 2.4). A correlation was observed in the yields of the low-molecular weight oil fractions and the general solubility of the lignin sample in the reaction solvent DMC. Organosolv cherry lignin had the lowest solubility in DMC and accordingly afforded the lowest low-molecular weight oil fraction (52 wt%). Table 5 summarises quantification results of the major mono-aromatic cleavage products (**2a,b** and **3a,b**) that we expected to find based on our model-based studies (Scheme 3). The product mixtures from oak, cherry, and beechwood lignin contained the capped syringaldehyde ester (**3b**) in major quantities while the capped guaiacyl ester yields remained within the expected product ratio (**2a,b** / **3a,b)**, corresponding well to the amount of S and G units in the lignin starting material (compare Tables 1 and 5). Because the Kraft lignin from Sigma Aldrich (#370959) almost exclusively contains G units, the S containing units were only observed in trace quantities. Additionally, various capped liner esters were observed in the oil fraction of the lignin samples (see Electronic Supplementary Information). Considering that the cost of the reagents can be a limiting factor for reaction scale up with regards to biorefinery application, we also performed the BCD reaction with a widely available Kraft lignin and KOH as base (Table 5, last column). To our delight, similar selectivities for the aromatic products were observed with comparable yields as to the Cs_2CO_3-catalysed reactions.

Depolymerisation of Beechwood Chips

After the successful degradation of extracted lignin samples, we decided to test the direct applicability of our BCD system on wood. The reaction was performed using a sample of pre-milled beechwood chips (100 mg) with Cs_2CO_3 (10 wt%) in DMC. Pleasingly an oil fraction of 40 wt% was recovered while affording a deep brown residue in 60 wt%. The oil fraction was then subject to GC-MS analysis (Fig. 4) and gratifyingly we could identify methoxy-capped monoaromatic products with a similar product distribution as observed for the extracted lignin samples. A control reaction carried out in the absence of base did not afford any cleavage products thereby ruling out any influence of the pre-milling conditions on the product formation (see Electronic Supplementary Information Fig. S9).

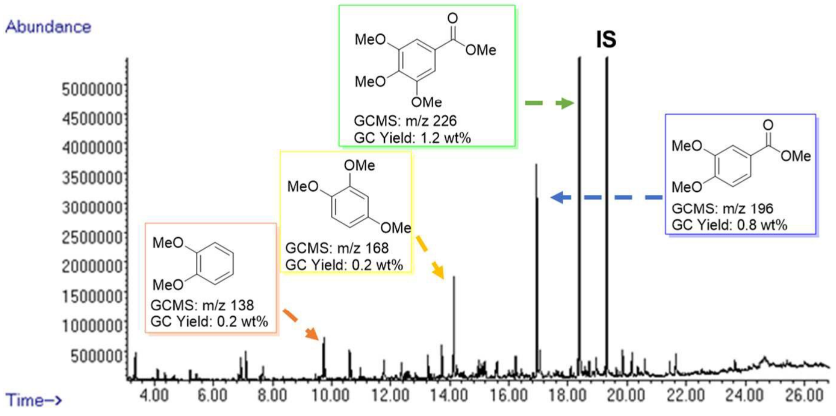

View Article Online
DOI: 10.1039/C7GC03110F

Fig. 4 GC-FID trace of the product mixture obtained from the depolymerisation of milled beechwood chips (100 mg) using Cs_2CO_3 (10 wt %) in DMC (5 mL) at 180 °C for 8 h. Identification of the major peaks is based on the GC-MS data (full peak overview in Table S6). Quantification is based on the standardization of individual products, using *n*-octadecane as an internal standard.

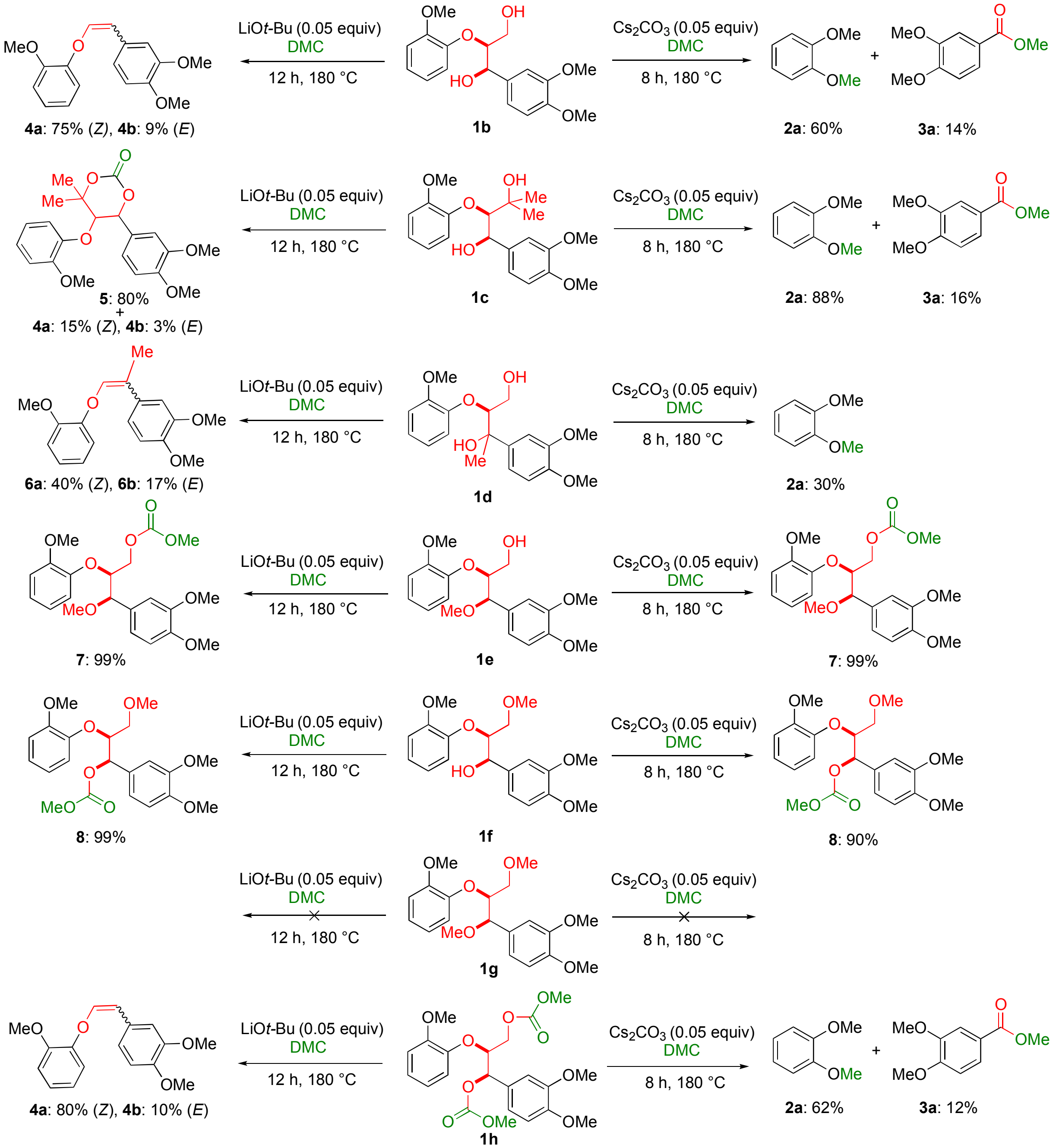

Scheme 3 Base-catalysed degradation in lignin *β*-O-4 model compounds.

Model compound studies

The obtained results for the BCD on lignin samples and wood gave rise to the question which reaction pathway is involved in the cleavage of the *β*-O-4 bonds and the subsequent capping of products. To answer this question a range of lignin *β*-O-4 model compounds were investigated having some of their pivotal sites such as the *α*-proton, *γ*-proton, or either one or both the aliphatic hydroxyls substituted by methyl or methoxy groups (Scheme 3). The idea was to compare the reactivity of these models (**1c**-**h**) with the unsubstituted model compound **1b**. Model compound **1c** which has both of its *γ*-protons replaced by methyl groups resulted in increased veratrole (**2a**) and dimethoxy benzoate (**3a**)

View Article Online
DOI: 10.1039/C7GC03110F

yields for the Cs_2CO_3-catalysed reaction. However, model **1d** containing the substituted α-proton formed a complex mixture of products with the overall yields for **2a** decreasing by half (30%). This loss in yield suggests a possible involvement of the α-proton in the cleavage reactions for **1b**. On the contrary, the reaction of both **1c** and **1d** with LiO*t*-Bu resulted in an overall decrease in yields for the corresponding alkenes **4** and **6** possibly due to the formation of an additional cyclic product such as **5**. Furthermore, substituting either one of the two aliphatic hydroxyls such as in model **1e** and **1f** restricted the reactions for both bases to stop at the monocarboxylated products **7** and **8**, thereby highlighting the necessity of both the positions to be free to initiate a successful cleavage and elimination reaction. This was further confirmed by model **1g** that remained unreactive for both base catalysts. Based on our observations on model compound studies (Scheme 4), the formation of dicarboxylated product **1h** starting from model **1b** in DMC was speculated to be a common intermediate for the pathways involving both Cs_2CO_3 and LiO*t*-Bu. Indeed, individual reactions of **1h** with these bases furnished comparable results as with **1b** affording slightly increased yields (Schemes 3 and 4).

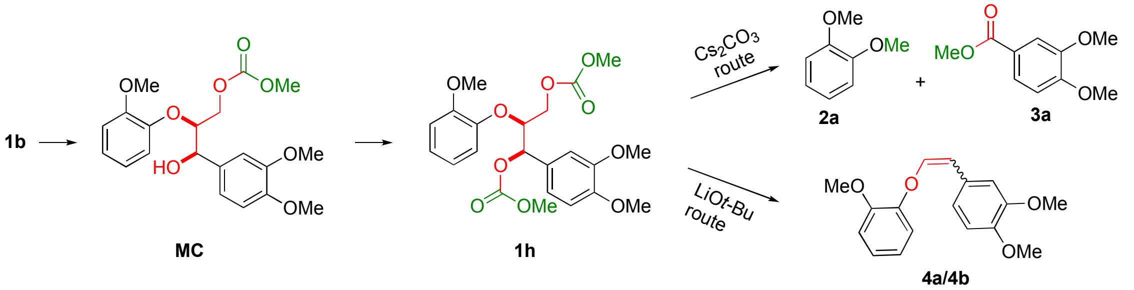

Scheme 4 Reaction of the β-O-4 model linkage under BCD conditions showing the reaction sequence and the point of divergence in reactivity for Cs_2CO_3 and LiO*t*-Bu.

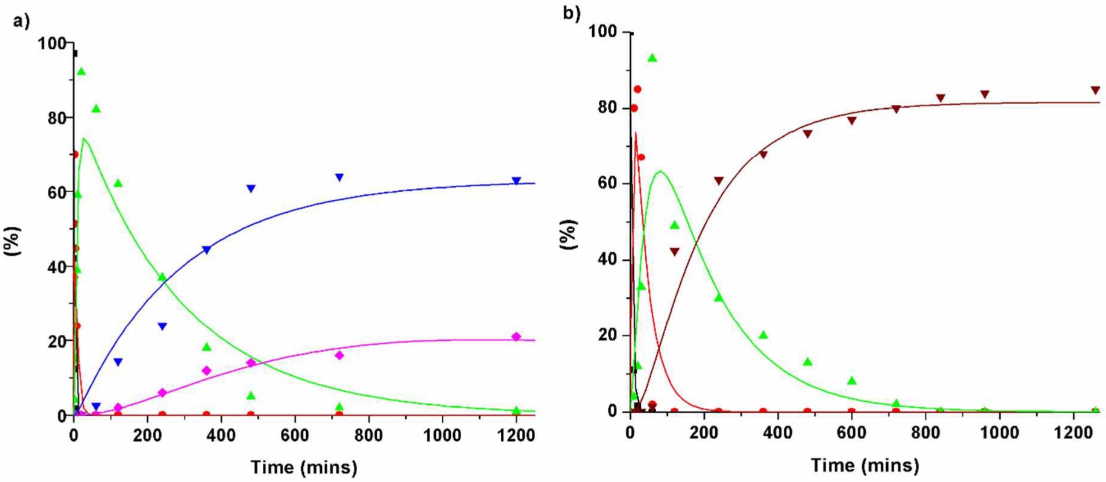

Fig. 5 Reaction profiles: a) Cs_2CO_3 180 °C in DMC with (β-O-4) model compound **1b**. b) LiO*t*-Bu 180 °C in DMC with (β-O-4) model compound **1b**. Dots show experimental data points, whereas the line is a modeled reaction. a) Black: dilignol (**1b**); Red: monocarboxylated dilignol (**MC**); Green: dicarboxylated dilignol (**1h**); Blue: veratrole (**2a**); Pink: 3,4-dimethoxy benzoate (**3a**). b) Black: dilignol (**1b**); Red: monocarboxylated dilignol (**MC**); Green: dicarboxylated dilignol (**Ih**); Brown: cis/trans alkenes (**4a**/**4b**).

Reaction Profile Study

To gain further insight into the degradation of the β-O-4 linkage under the Cs_2CO_3- and LiO*t*-Bu-catalysed reaction conditions, the consumption of **1b** and the formation of stable intermediates and products was monitoring by HPLC analysis (Fig. 5, see Electronic Supplementary Information section 4). From this analysis, a series of reaction pathways were proposed, and rate analysis provided the curve fits shown in corresponding figures.

The initial reactions were found to be the same for both Cs_2CO_3 and LiO*t*-Bu. Carboxylation of the γ-hydroxy group occurred first (reaction rates of **MC** = 0.69 min^{-1} for Cs_2CO_3 and 0.2 min^{-1} for LiO*t*-Bu) followed by a second carboxylation of the α-hydroxy group resulting in common intermediate **1h** (reaction rates of **1h** = 0.15 min^{-1} for Cs_2CO_3 and 0.025 min^{-1} for LiO*t*-Bu). Following the formation of **1h,** the reaction pathways diverge. The reaction with Cs_2CO_3 promotes the cleavage of the C-O bond resulting in veratrole (**2a**). The production of **2a**, however, does not correlate directly with the accruement of 3,4-dimethoxy benzoate (**3a**). A probable intermediate **M** is speculated to be formed which undergoes a subsequent reacion to **3a**. The detailed reaction pathway leading to **M** is discussed later during the computational analysis.

Upon the formation of **1h** in the reaction with LiO*t*-Bu, the alkenes **4a** and **4b** are formed without any

View Article Online
DOI: 10.1039/C7GC03110F

observable intermediates (rate of formation of **4a**/**4b** = 0.005 min^{-1}).

Computational Study

Based on the studies above, quantum chemical calculations were considered necessary to find a reasonable mechanism rationalising the observed selectivities for the obtained cleavage products. Here again dilignol **1b** was chosen as representative substrate and cesium methanolate (CsOMe) as a model base considering the depletion of Cs_2CO_3 (0.05 equiv) over the course of the reaction resulting in methanolate as by-product.

Thus, after an initiation period mainly methanolates acted as a base in the reaction. The investigated reaction pathways were limited to intermediates and transition states without explicit coordination of the cesium ions. The main reason for this approximation being the dramatically increased number of different structures and possible oligomers that would have to be taken into consideration for each step. Secondly, the PCM solvation model would be inaccurate for the description of the solvated species in this system preventing a reliable comparison of structures with different coordination of the cesium cation. Also, based on Pearson's HSAB principle, it can be expected that the uncoordinated intermediates and transition states provide a good correlation for the reactions with a cesium base owing to its weak coordination to the deprotonated oxygen atoms of the substrate.[14]

The model compound studies (Scheme 3) suggest the involvement of both the α- and γ-protons in the formation of veratrole (**2a**) and 3,4-dimethoxy benzoate (**3a**). The decreased yield of **2a** for model compound **1d** specifically indicates that these reaction products are formed after a deprotonation at the α-position. This deprotonation reaction, however, is most likely occurring on the dicarboxylated dilignol **1h** since, in contrast to **1b**, it has no free hydroxy groups, which are more acidic than the aliphatic hydrogen atoms. Moreover, the experimental results already indicate **1h** as an intermediate in the formation of **2a** and **3a** (see Scheme 3; reaction of **1h** with Cs_2CO_3 and Fig. 5a).

The deprotonation at the α-carbon of **1h** results in intermediate **M1** (Scheme 5). This intermediate is favoured with a Gibbs energy difference of 15.2 kcal mol^{-1} over **M1b** which is deprotonated at the γ-carbon. The energy of **M1** is 36.9 kcal mol^{-1} relative to **1b**. The transition state of the deprotonation (**TS-1**) has a Gibbs energy of 37.2 kcal mol^{-1} relative to **1b**. The elimination of guaiacolate (**11**) from **M1** proceeds without a significant barrier and gives enol ether **M2**. The formation of veratrole from **1d** (Scheme 3) can be attributed to a deprotonation at the γ-position. However, the lower acidity of the hydrogen at the γ-position compared to the one in α-position explains the low yield for veratrole (**2a**). Furthermore, the absence of **3a** in the product spectrum of **1d** can be explained by the formation of a different intermediate after the elimination process. Additionally, a similar product inhibition for the formation of veratrole by *o*-methoxy groups was also observed in our previous study.[10p] The overall change of the selectivity thus indicates that the steric hindrance at the α-carbon might be preventing the deprotonation.

Based on a recent computational study by Yu,[15] we also investigated a possible elimination of guaiacolate from the monocarboxylated structure **M9** resulting in an oxirane intermediate (see Scheme 6). However, the Gibbs energy of the transition state **TS-9** of this reaction is 69.4 kcal mol^{-1} relative to **1b** and 32.2 kcal mol^{-1} relative to **TS-1**. Therefore, Yu's mechanism is highly disfavoured in our reaction system.

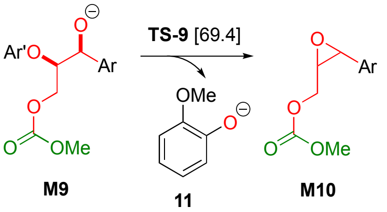

Scheme 6 Elimination of **11** According to Yu *et al.*[15]; Ar: 3,4-dimethoxyphenyl; Ar': 2-methoxyphenyl; [Relative Gibbs Energies to **1b** in kcal mol^{-1}].

The final step for the formation of **2a** is the methylation of **11** by dimethyl carbonate. The relative Gibbs energy of the transition state of the methylation under Walden inversion at the methyl group is 24.5 kcal mol^{-1} relative to **11**.

The formation of **3a** is a result of the decomposition of **M2**. The addition of a methanolate to the methoxy carbonate group is endergonic. The resulting intermediate **M3** has a Gibbs energy of 19.6 kcal mol^{-1} relative to **M2**. The transition state of this step has an energy of 33.8 kcal mol^{-1} compared to **M2**. Elimination of dimethyl carbonate from **M3** results in a simultaneous elimination of monomethoxy carbonate (**MMC**, decomposing into MeOH and CO_2). The transition state **TS-4** of this step is only 2.0 kcal mol^{-1} higher in energy than **M3**. Moreover, the reaction is highly exergonic since the Gibbs energy of the vinyl ketone **M4** is 74.6 kcal mol^{-1} lower than **M3** and the energy is 55.0 kcal mol^{-1} lower than **M2.** The vinyl ketone **M4** can react with methanolate to give the enolate **M5**. The addition reaction is endergonic with an energy difference of 13.9 kcal mol^{-1} and the corresponding transition state **TS-5** having an energy of 37.2 kcal mol^{-1}. Addition of dimethyl carbonate to the α-carbon of **M5** in a Claisen condensation-type reaction (**TS-6**) results in intermediate **M6**. Instead of an elimination of a methanolate, a transfer of a methoxy group of the dimethyl carbonate group to the carbonyl group is likely to occur. The resulting intermediate **M7** resembles the intermediate of a Claisen condensation between 3,4-dimethoxy benzoate and the enolate **M8**. Hence, a retro-Claisen condensation-type step (**TS-8**) yields the experimentally observed product **3a**. The formation of **3a** and **M8** is highly exergonic with an energy difference

View Article Online
DOI: 10.1039/C7GC03110F

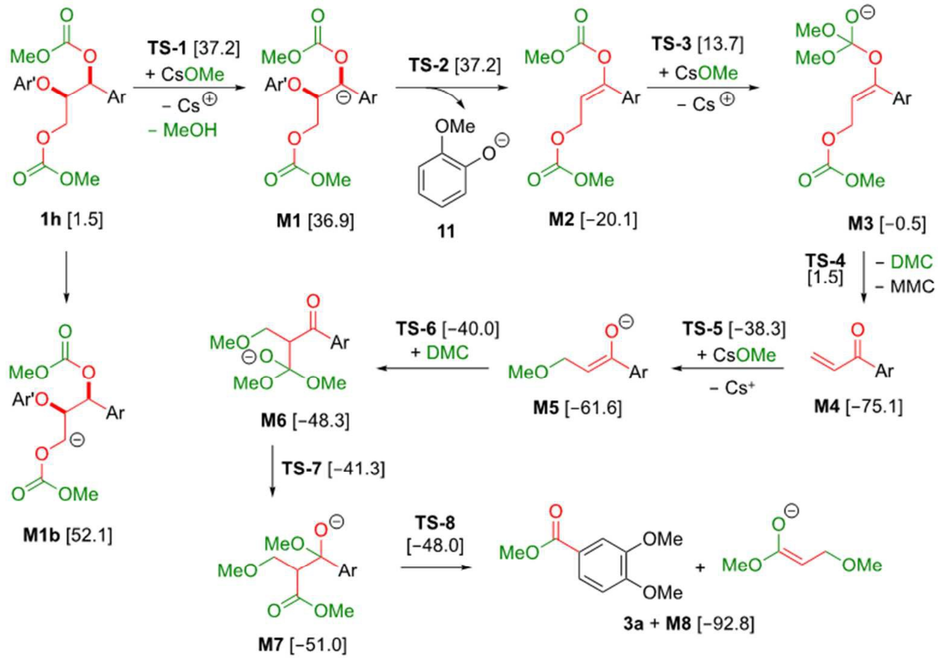

Scheme 5 Reaction pathway from dicarboxylated Dilignol **1h** to 3,4-dimethoxy benzoate (**3a**); Ar: 3,4-dimethoxyphenyl; Ar': 2-methoxyphenyl; **MMC**: monomethoxy carbonate; [Gibbs Energies Relative to **1b** in kcal mol^{-1}]

of 92.8 kcal mol^{-1} relative to **4a** and 17.7 kcal mol^{-1} relative to **M4**. **TS-5** is the transition state with the highest Gibbs energy (35.1 kcal mol^{-1} relative to **M4**) between **M4** and **3a**. To support the proposed reaction pathway, we investigated a crucial intermediate: the vinyl ketone **M4** (Scheme 7). **M4** was synthesised (see Electronic Supplementary Information 5) and used as a starting material in a reaction under the same conditions as shown for **1b** in Scheme 3.

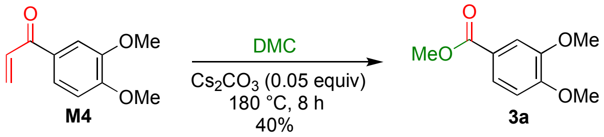

Scheme 7 Reaction of **M4** with Cs_2CO_3 in DMC.

The formation of **3a** in 40% yield when employing **M4** as starting material confirms that there is a reaction pathway between **M4** and **3a**. This is also in accordance with the proposed formation of an intermediate **M** while studying the reaction profile for the decomposition of **1b** with caesium carbonate to **3a** (Electronic Supplementary Information section 4.3; **M** = **M4**).

Conclusion

We have developed a base-catalysed depolymerisation strategy for various lignin samples including organosolv and Kraft lignin in dimethyl carbonate using alkaline earth metal catalysts. For the first time, a truly catalytic base-catalysed depolymerisation process (catalyst loadings of around 5 mol%) is demonstrated affording low-molecular weight oils. For all lignin sample, the low-molecular weight oil and the ethyl acetate insoluble fractions were quantified and characterised using HSQC 2D-NMR, ^{31}P NMR, GPC, and GC-MS measurements. The oil fractions for the Cs_2CO_3-catalysed lignin degradation were found to be within the range of 52-67 wt% of the starting lignin material and contained a range of methoxy capped aromatic monomers. Furthermore, it was shown that for potential future biorefinery applications the base can be changed to readily available KOH affording similar monomer yields. The methodology with the caesium salt was also effective for the direct degradation of milled beechwood chips thereby further expanding the scope on a more robust lignocellulosic starting material. These results are well in agreement with our model compound studies and hence prove the system's efficiency and applicability to the complex lignin polymer. In our quest to understand the different reaction pathway involved in the degradation using LiO*t*-Bu and Cs_2CO_3 in dimethyl carbonate, we further studied a variety of lignin model compounds (**1a-1h**), which demonstrated the importance of the free aliphatic hydroxy groups and the proton at α-carbon of the lignin β-O-4 linkage in the depolymerisation reaction. Monitoring the reaction of **1b** for both bases helped to elucidate the overall reaction pathway and the point of divergence for the bases that leads to the different product selectivities. This was further confirmed by the quantum chemical calculations performed for the Cs_2CO_3-catalysed cleavage reaction on model compound **1b**. Ultimately, we could provide a rational reaction pathway for our BCD system in dimethyl carbonate based upon our extensive studies on both model compound and real lignin samples.[17]

Conflicts of interest

There are no conflicts to declare.

Acknowledgements

This research was supported by the European Commission (SuBiCat Initial Training Network, Call FP7-PEOPLE-2013-ITN, grant no. 607044). S. D., S. S. M. S., and C. W. L. thank the international training network SubiCat for their predoctoral stipends. J. M. is grateful to the NRW Graduate School BrenaRo and the German Academic Exchange Service (DAAD) for predoctoral stipends. J. E. thanks the Deutsche Forschungsgemeinschaft through the International Research Training Group Seleca (IGRK 1628) and the IT Center of RWTH Aachen University for providing the computational resources. We thank Dr. N. Anders (RWTH Aachen University) for the GPC measurements, T. Rinesch (RWTH Aachen University) for proofreading the manuscript, Dr. C. Räuber (RWTH Aachen University) for helpful discussions during the NMR investigations. Prof. Dr. Paul C. J. Kamer, Prof. Dr. Andrew D. Smith, Prof. Dr. Nick Westwood (all University of St Andrews, Scotland) and Dr. R. Rinaldi (formerly MPI für Kohlenforschung, Mülheim a.d.R.) are acknowledged for their helpful discussions and for supplying Oak, Cherry and Beechwood lignin samples, respectively.

Notes and references

1 (*a*) A. Sakakibari, *Wood Sci. Technol.*, 1980, **14**, 89–100; (*b*) R. D. Perlack, L. L. Wright, A. F. Turhollow, R. L. Graham, B. J. Stokes, D. C. Erbach, U. S. Department of Energy, Biomass as Feedstock for a bioenergy and bioproducts industry: the technical feasibility of a billion-ton annual supply, 2005.

2 (*a*) J. Zakzeski, P. C. A. Bruijnincx, A. L. Jongerius and B. M. Weckhuysen, *Chem. Rev.*, 2010, **110**, 3552−3599; (*b*) A. J. Ragauskas, G. T. Beckham, M. J. Biddy, R. Chandra, F. Chen, M. F. Davis, B. H. Davison, R. A. Dixon, P. Gilna, M. Keller, P. Langan, A. K. Naskar, J. N. Saddler, T. J. Tschaplinski, G. A. Tuskan and C. E. Wyman, *Science*, 2014, **344**, 1246843; (*c*) M. D. Karkas, B. S. Matsuura, T. M. Monos, G. Magallanes and C. R. Stephenson, *Org. Biomol. Chem.*, 2016, **14**, 1853−1914; (*d*) S. Dabral, M. Turberg, A. Wanninger, C. Bolm, and J. G. Hernández, *Molecules*, 2017, **22**, 146.

3 (*a*) C. Li, X. Zhao, A. Wang, G. W. Huber and T. Zhang, *Chem. Rev.*, 2015, **115**, 11559−11624; (*b*) D. Kai, M. J. Tan, P. L. Chee, Y. K. Chua, Y. L. Yap and X. J. Loh, *Green Chem.*, 2016, **18**, 1175−1200.

4 (*a*) P. J. Deuss, K. Barta and J. G. de Vries, *Catal. Sci. Technol.*, 2014, **4**, 1174–1196; (*b*) C. Xu, R. A. D. Arancon, J. Labidi and R. Luque, *Chem. Soc. Rev.*, 2014, **43**, 7485−7500; (*c*) R. Rinaldi, R. Jastrzebski, M. T. Clough, J. Ralph, M. Kennema, P. C. A. Bruijnincx and B. M. Weckhuysen, *Angew. Chem. Int. Ed.*, 2016, **55**, 8164−8215; (*d*) U. Weißbach, S. Dabral, L. Konnert, C. Bolm and J. G. Hernández, *Beilstein J. Org. Chem.*, 2017, **13**, 1788−1795; (*e*) S. Gillet, M. Aguedo, L. Petitjean, A.R. C. Morais, A. M. da Costa. Lopes, R. M. Łukasik and P. T. Anastas, *Green Chem*., 2017, **19**, 4200−4233.

5 Selected oxidative degradation approach *via* benzylic alcohol oxidation: (*a*) A. Wu, B. O. Patrick, E. Chung and B. R. James, *Dalton Trans*., 2012, **41**, 11093–11106; (*b*) A. Rahimi, A. Azarpira, H. Kim, J. Ralph and S. S. Stahl, *J. Am. Chem. Soc.*, 2013, **135**, 6415–6418; (*c*) J. D. Nguyen, B. S. Matsuura and C. R. J. Stephenson, *J. Am. Chem. Soc.*, 2014, **136**, 1218–122; (*d*) A. Rahimi, A. Ulbrich, J. J. Coon and S. S. Stahl, *Nature*, 2014, **515**, 249–252; (*e*) K. Walsh, H. F. Sneddon and C. J. Moody, *Org. Lett*., 2014, **16**, 5224−5227; (*f*) M. Dawange, M. V. Galkin and J. S. M. Samec, *ChemCatChem*, 2015, **7**, 401–404; (*g*) C. S. Lancefield, O. S. Ojo, F. Tran and N. J. Westwood, *Angew Chem. Int. Ed.*, 2015, **54**, 258–262; (*h*) R. Zhu, B. Wang, M. Cui, J. Deng, X. Li, Y. Ma and Y. Fu, *Green Chem.*, 2016, **18**, 2029–2036; (*i*) S. Dabral, J. G. Hernández, P. C. J. Kamer and C. Bolm, *ChemSusChem* 2017, **10**, 2707–2713.

6 For selected articles see: (*a*) S. K. Hanson, R. T. Baker, J. C. Gordon, B. L. Scott and D. L. Thorn, *Inorg. Chem*., 2010, **49**, 5611–5618; (*b*) S. Son and F. D. Toste, *Angew. Chem. Int. Ed*., 2010, **49**, 3791–3794; (*c*) J. Zakzeski, P. C. A. Bruijnincx and B. M. Weckhuysen, *Green Chem.*, 2011, **13**, 671–680; (*d*) B. Sedai, C. Díaz-Urrutia, R. T. Baker, R. Wu, L. A. Pete Silks and S. K. Hanson, *ACS Catal.*, 2011, **1**, 794–804; (*e*) S. K. Hanson, R. Wu and L. A. Pete Silks, *Angew. Chem. Int. Ed.*, 2012, **51**, 3410–3413; (*f*) B. Biannic and J. J. Bozell, *Org. Lett.*, 2013, **15**, 2730–2733; (*g*) J. M. W. Chan, S. Bauer, H. Sorek, S. Sreekumar, K. Wang and F. D. Toste, *ACS Catal.*, 2013, **3**, 1369–1377; (*h*) B. Sedai and T. Baker, *Adv. Synth. Catal.*, 2014, **356**, 3563–3574; (*i*) J. Mottweiler, M. Puche, C. Räuber, T. Schmidt, P. Concepción, A. Corma and C. Bolm, *ChemSusChem*, 2015, **8**, 2106–2113; (*j*) J. Mottweiler, T. Rinesch, C. Besson, J. Buendia and C. Bolm, C. *Green Chem*., 2015, **17**, 5001–5008; (*k*) T. Rinesch, J. Mottweiler, M. Puche, C. Räuber, T. Schmidt, P. Concepción, A. Corma and C. Bolm, *ACS Sustainable Chem. Eng.*, 2017, **5**, 9818-9825.

7 For selected articles see: (*a*) N. Yan, C. Zhao, P. J. Dyson, C. Wang, L. Liu, and Y. Kou, *ChemSusChem*, 2008, **1**, 626–629; (*b*) A. G. Sergeev and J. F. Hartwig *Science*, 2011, **332**, 439–443; (*c*) A. L. Jongerius, R. Jastrzebski, P. C. A. Bruijnincx and B. M. Weckhuysen, *J. Catal*., 2012, **285**, 315–323; (*d*) J. Zakzeski, A. L. Jongerius, P. C. A. Bruijnincx and B. M. Weckhuysen, *ChemSusChem*, 2012, **5**, 1602–1609; (*e*) A. G. Sergeev, J. D. Webb and J. F. Hartwig, *J. Am. Chem. Soc*., 2012, **134**, 20226–20229; (*f*) J. He, C. Zhao and J. A. Lercher, *J. Am. Chem. Soc.*, 2012, **134**, 20768–20775; (*g*) Z. Strassberger, A. H. Alberts, M. J. Louwerse, S. Tanase and G. Rothenberg, *Green Chem*., 2013, **15**, 768–774; (*h*) T. H. Parsell, B. C. Owen, I. Klein, T. M. Jarrell, C. L. Marcum, L. J. Haupert, L. M. Amundson, H. I. Kenttämaa, F. Ribeiro, J. T. Miller, and M. M. AbuOmar, M. M. *Chem. Sci*., 2013, **4**, 806–813; (*i*) J. A. Barrett, Y. Gao, C. M. Bernt, M. Chui, A. T. Tran, M. B. Foston and P. C. Ford, *ACS Sustainable Chem. Eng.*, 2016, **4**, 6877−6886.

8 For selected articles see: (*a*) M. Nagy, K. David, G. J. P. Britovsek and A. J. Ragauskas, *Holzforschung*, 2009, **63**, 513–520; (*b*) J. M. Nichols, L. M. Bishop, R. J. Bergman and J. A. Ellman, *J. Am. Chem. Soc.*, 2010, **132**, 12554–12555; (*c*) T. vom. Stein, T. Weigand, C.

Merkens, J. Klankermayer and W. Leitner, *ChemCatChem*, 2013, **5**, 439–441; (*d*) D. Weickmann and B. Plietker, *ChemCatChem*, 2013, **5**, 2170–2173; (*e*) R. G. Harms, I. I. E. Markovits, M. Drees, W. A. Herrmann, M. Cokoja and F. E. Kìhn, *ChemSusChem*, 2014, **7**, 429–434; (f) T. vom. Stein, T. den. Hartog, J. Buendia, S. Stoychev, J. Mottweiler, C. Bolm, J. Klankermayer and W. Leitner, W. *Angew. Chem. Int. Ed.*, 2015, **54**, 5859–5863.

9 For selected recent articles see: (*a*) S. Jia, B. J. Cox, X. Guo, Z. C. Zhang and J. G. Ekerdt, *ChemSusChem*, 2010, **3**, 1078− 1084; (*b*) M. R. Sturgeon, S. Kim, K. Lawrence, R. S. Paton, S. C. Chmely, M. Nimlos, T. D. Foust and G. T. Beckham, *ACS Sustainable Chem. Eng.*, 2014, **2**, 472−485; (*c*) T. Yokoyama, *J. Wood Chem. Technol.*, 2014, **35**, 27−42; (*d*) R. G. Harms, I. I. E. Markovits, M. Drees, W. A. Herrmann, M. Cokoja and F. E. Kühn, *ChemSusChem*, 2014, **7**, 429−434; (*e*) A. Kaiho, M. Kogo, R. Sakai, K. Saito and T. Watanabe, *Green Chem.*, 2015, **17**, 2780−2783; (*f*) P. J. Deuss, M. Scott, F. Tran, N. J. Westwood, J. G. de Vries and K. Barta, *J. Am. Chem. Soc.*, 2015, **137**, 7456−7467; (*g*) M. Scott, P. J. Deuss, J. G. de Vries, M. H. G. Prechtl and K. Barta, *Catal. Sci. Technol.*, 2016, **6**, 1882−1891; (*h*) C. W. Lahive, P. J. Deuss, C. S. Lancefield, Z. Sun, D. B. Cordes, C. M. Young, F. Tran, A. M. Z. Slawin, P. C. J. Kamer, J. G. de Vries, N. J. Westwood and K. Barta, *J. Am. Chem. Soc.*, 2016, **138**, 8900−8911.

10 For homogeneous base-catalysed degradation of lignin model compounds and lignin see: (*a*) R. W. Thring, *Biomass Bioenergy*, 1994, **7**, 125–130; (*b*) J. E. Miller, I. Evans, A. Littlewolf and D. E. Trudell, *Fuel*, 1999, **78**, 1363–1366; (*c*) J.S. Shabtal, W. W. Zmierczak and E. Chornet, Process for conversion of lignin to reformulated, partially oxygenated gasoline. U. S. Patent US 6,172,272 B1, Jan. 9, 2001; (*d*) J. S. Shabtal, W. W. Zmierczak, E. Chornet and D. Johnson, Process for converting lignins into a high octane blending component. U. S. Patent US 2003/0115792 A1, June 26, 2003; (*e*) J. S. Shabtal, W. W. Zmierczak, E. Chornet and D. Johnson, Process for converting lignins into a high octane additive. U. S. Patent US 2003/0100807 A1, May 29, 2003; (*f*) S. Karagöz, T. Bhaskar, A. Muto and Y. Sakata, *Fuel*, 2004, **83**, 2293–2299; (*g*) A. Vigneault, D. K. Johnson and E. Chornet, *Can. J. Chem. Eng*., 2007, **85**, 906–916; (*h*) S. Nenkova, T. Vasileva and K. Stanulov, *Chem. Nat. Compd*., 2008, **44**, 182–185; (*i*) J. M. Lavoie, W. Baré and M. Bilodeau, *Bioresour. Technol*., 2011, **102**, 4917–4920; (*j*) V. M. Roberts, V. Stein, T. Reiner, A. Lemonidou, X. Li and J. A. Lercher, *Chem. Eur. J*., 2011, **17**, 5939–5948; (*k*) R. Beauchet, F. Monteil-Rivera and J. M. Lavoie, *Bioresour. Technol*., 2012, **121**, 328–334; (*l*) A. Toledano, L. Serrano and J. Labidi, *J. Chem. Technol. Biotechnol*., 2012, **87**, 1593–1599; (*m*) T. Kleine, J. Buendia and C. Bolm, *Green Chem*., 2013, **15**, 160–166; (*n*) A. Toledano, L. Serrano and J. Labidi, *Fuel*, 2014, **116**, 617–624; (*o*) E. M. Karp, B. S. Donohoe, M. H. O'Brien, P. N. Ciesielski, A. Mittal, M. J. Biddy, and G. T. Beckham, *ACS Sustainable Chem. Eng.*, 2014, **2**, 1481–1491; (*p*) S. Dabral, J. Mottweiler, T. Rinesch and C. Bolm, *Green Chem.*, 2015, **17**, 4908−4917. (*q*) R. Katahira, A. Mittal, K. Mc Kinney, X. Chen, M. P. Tucker, D. K. Johnson and G. T. Beckham, *ACS Sustainable Chem. Eng.*, 2016, **4**, 1474−1486; (*r*) A. Rodriguez, D. Salvachúa, R. Katahira, B. A. Black, N. S. Cleveland, M. Reed, H. Smith, E. E. K. Baidoo, J. D. Keasling, B. A. Simmons, G. T. Beckham and J. M. Gladden, *ACS Sustainable Chem. Eng.*, 2017, **5**, 8171−8180; (*s*) Z. Strassberger, P. Prinsen, F. vam der Klis, D. S. van Es, S. Tanase and G. Rothenberger, *Green Chem*., 2015, **17**, 325-334.

11 For heterogeneous base-catalysed degradation of lignin model compounds and lignin see: (*a*) G. S. Macala, T. D. Matson, C. L. Johnson, R. S. Lewis, A. V. Iretskii and P. C. Ford, *ChemSusChem*, 2009, **2**, 215–217; (*b*) Z. Yuan, S. Cheng, M. Leitch and C. C. Xu, *Bioresour. Technol*., 2010, **101**, 9308–9313; (*c*) M. R. Sturgeon, M. H. O'Brien, P. N. Ciesielski, R. Katahira, J. S. Kruger, S. C. Chmely, J. Hamlin, K. Lawrence, G. B. Hunsinger, T. D. Foust, R. M. Baldwin, M. J. Biddy and G. T. Beckham, *Green Chem*., 2014, **16**, 824–835; (*d*) K. Barta, G. R. Warner, E. S. Beach and P. T. Anastas, *Green Chem*., 2014, **16**, 191–196; (*e*) J. Long, Q. Zhang, T. Wang, X. Zhang, Y. Xu and L. Ma, *Bioresour. Technol*., 2014, **154**, 10–17; (*f*) J. S. Kruger, N. S. Cleveland, S. Zhang, R. Katahira, B. A. Black, G. M. Chupka, T. Lammens, P. G. Hamilton, M. J. Biddy and G. T. Beckham, *ACS Catal.*, 2016, **6**, 1316–1328; (*g*) R. Chaudhary and P. L. Dhepe, *Green Chem.*, 2017, **19**, 778– 788.

12 (*a*) D. S. Argyropoulos, *Res. Chem. Intermed*., 1995, **21**, 373–395; (*b*) Y. Pu, S. Cao and A. J. Ragauskas, *Energy Environ. Sci.*, 2011, **4**, 3154–3166; (*c*) M. Balakshin and E. Capanema, *J. Wood Chem. Technol*., 2015, **35**, 220–237; (*d*) S. Constant, H. L. J. Wienk, A. E. Frissen, P. de. Peinder, R. Boelens, D. S. van Es, R. J. H. Grisel, B. M. Weckhuysen, W. J. J. Huijgen, R. J. A. Gosselink and P. C. A. Bruijnincx, *Green Chem*., 2016, **18**, 2651–2665.

13 (*a*) S. Ouk, S. Thiebaud, E. Borredon, P. Legars and L. Lecomte, *Tetrahedron Lett*., 2002, **43**, 2661–2663; (*b*) K. M. Deshmukh, Z. S. Qureshi, K. P. Dhake and B. M. Bhanage, *Catalysis Comm*., 2010, **12**, 207–211; (*c*) J. N. G. Stanley, M. Selva, A. F. Masters, T. Maschmeyerb and A. Perosa, *Green Chem*., 2013, **15**, 3195–3204.

14 R. G. Pearson, *J. Am. Chem. Soc.*, 1963, **85**, 3533−3539.

15 T. Lankau and C. H. Yu, *Green Chem.*, 2016, **18**, 1590−1596.

16 (*a*) J. Gierer, *Wood Sci. Technol.*, 1980, **14**, 241−266. (*b*) H. Kawamoto, S. Horigoshi and S. Saka, *J. Wood Sci.*, 2006, **53**, 168−174.

17 For two very instructive reviews on the use of DMC, which were published during the evaluation of this manuscript, see: (*a*) P. Tundo, M. Musolino and F. Aricò, *Green Chem.*, DOI: 10.1039/c7gc01764b; (*b*) G. Fiorani, A. Perosa and M. Selva, *Green. Chem.*, DOI: 10.1039/c7gc02118f.

View Article Online
DOI: 10.1039/C7GC03110F

TOC

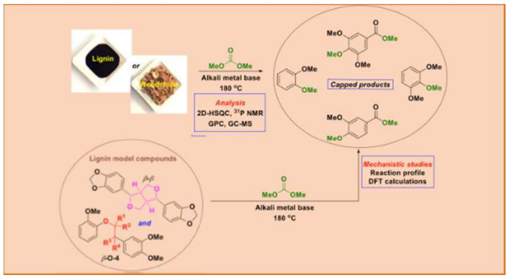

Text:

Various analytical techniques and DFT calculations have been applied in studying base-catalysed lignin degradations in dimethyl carbonate.

View Article Online
DOI: 10.1039/C7GC03110F

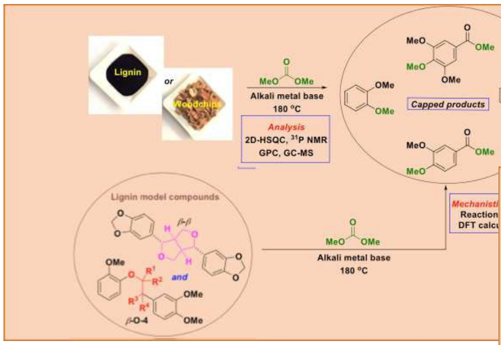

Various analytical techniques and DFT calculations have been applied in studying base-catalysed lignin degradations in dimethyl carbonate.